Eur. Phys. J. A **31**, 665–671 (2007)
DOI 10.1140/epja/i2006-10283-5

THE EUROPEAN PHYSICAL JOURNAL A

Special Article – QNP 2006

Unraveling the f_0 nature by connecting KLOE and BABAR data through analyticity

S. Pacetti[a]

Laboratori Nazionali di Frascati, INFN, Frascati, Italy

Received: 18 December 2006
Published online: 23 March 2007 –

Abstract. We define a general procedure, based on analyticity and dispersion relations, to estimate low-energy amplitudes for processes like: $\phi \to e^+e^- M$ and $\phi \to \gamma M$, starting from cross-section data on $e^+e^- \to \phi M$, where M is a generic light scalar or pseudoscalar meson. In particular this procedure is constructed to obtain predictions on the radiative decay rate which are crucially linked on the assumed quark structure for the meson M under consideration. Three cases are analyzed: $M = \eta$, $M = f_0(q\overline{q})$ and $M = f_0(qq\overline{qq})$. While in the η case the estimate of the branching fraction for the radiative decay $\phi \to \eta\gamma$ is in agreement with the data, in the case of f_0, such agreement is obtained only under the hypothesis of a tetraquark scalar meson.

PACS. 11.55.-n S-matrix theory; analytic structure of amplitudes – 13.25.-k Hadronic decays of mesons – 13.40.Gp Electromagnetic form factors

1 Introduction

1.1 The known properties of the $f_0(980)$ scalar meson

The $f_0(980)$ is the more extensively studied isospin zero scalar meson [1]. The properties of such a meson are very peculiar and, in some cases, in spite of the deep experimental investigation, they are still poorly known. In fact, while the mass is rather well measured $M_{f_0} = 980 \pm 10\,\text{MeV}$ [1], the width is known with a large uncertainty: $\Gamma_{f_0} = 40$–$100\,\text{MeV}$ [1]. This is a consequence of the scalar nature of this meson, which does not allow unambiguous interpretations when the resonance is studied by means of the usual Breit-Wigner analysis. The f_0 has the quantum number of the vacuum, the Higgs boson and also of the expected lowest-lying glueball [2].

Usually, this scalar meson is considered as a "bridge" between light (u and d) and strange quarks because it can be produced by both strange and non-strange particles.

1.2 Long outstanding questions

By following the standard quark model [1], where mesons are described as colorless $q\overline{q}$ bound states and classified in J^{PC} multiplets, we expect there should be the conventional flavor $SU(3)$ scalar nonet (0^{++}):

$$q^3 \otimes \overline{q}^{\overline{3}} = [\overline{q}q]^1 \oplus [\overline{q}q]^8. \quad (1)$$

In such a scenario the f_0 represents the singlet and, due to the large $s\overline{s}$ component, it should be the heaviest meson of this multiplet, in contradiction with the experimental data which provide: $M_{f_0} \simeq M_{a_0}$ and no degeneracy between a_0 and σ_0 ($M_{a_0} > M_{\sigma_0} \sim 450\,\text{MeV}$). Also the absolute values of the masses are not in agreement with the expectation, in fact, being $q\overline{q}$ bound in P-wave, these masses should lie in the $> 1\,\text{GeV}$ energy region of other P-wave states. This means that the $q\overline{q}$ bound state is only a small component of the f_0 Fock space.

Since some years, the interpretations in terms of tetraquark states (in different combinations) [3–9] is the object of deep theoretical and experimental investigation and also in this work we will focus on this possibility.

2 Probing the intrinsic nature of f_0

2.1 Common practice

At present, the main source of information on the f_0 structure is the radiative decay $\phi \to f_0\gamma$ [9], whose surprisingly high branching fraction is interpreted in terms of an abnormally strong affinity between the ϕ vector meson and the f_0 itself. Such an affinity has been described in different ways by different authors, even though, each of them put the cue on the key role played by the coupling $g^{f_0}_{KK}$. In particular, there are two schools of thought, the first one describes this coupling by introducing in the $\phi \to f_0\gamma$ amplitude a $K\overline{K}$-loop [3], while the second, in order to

[a] e-mail: simone.pacetti@lnf.infn.it

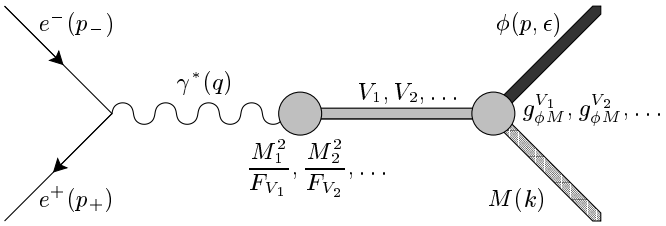

Fig. 1. Feynman diagram for the $e^+e^- \to \phi M$ in Born approximation, with intermediate vector mesons V_j.

avoid any model-dependent description, adopts a usual parameterization in terms of meson propagators with free couplings [6]. In both these descriptions, with different languages, the message is the same: the coupling $(g^{f_0}_{KK})^2$ is more than twice the $(g^{f_0}_{\pi\pi})^2$ [10].

2.2 The strategy

The idea of this work consists in probing the intrinsic nature of the f_0 by considering different processes to investigate the transition form factor (tff) which describes the coupling $\phi f_0 \gamma$. All the information on the tff are then used under the constraint of an assumed f_0 quark structure, which strongly affects every step of the procedure.

3 First step: parameterization in the resonance region [$3M_\pi, \sim 3$ GeV]

The amplitude of $e^+e^- \to \phi M$ (fig. 1) is parameterized in terms of a tff, which describes the coupling between the virtual photon and the intermediate vector mesons V_j, *i.e.*:

$$\mathcal{M}_{\rm Annihi} = \sum_j^{N_V} \frac{g^{V_j}_{\phi M}}{M_j^2 - q^2 - i\Gamma_j M_j} \frac{M_j^2}{F_{V_j}} \epsilon_\nu \mathcal{T}_M^{\mu\nu} \frac{1}{q^2} J_\mu, \quad (2)$$

where $J_\mu = -ie\overline{v}(p_+)\gamma_\mu u(p_-)$, ϵ_ν is the ϕ polarization vector and, F_{V_j} and $g^{V_j}_{\phi M}$ are couplings with the initial and the final state. The second-rank tensors $\mathcal{T}_M^{\mu\nu}$ accounts for the dynamics of the meson M.

The formal expression of the ϕM tff, in the resonance region, as extracted from the amplitude of eq. (2), is

$$F^{\rm Res}_{\phi M}(q^2) = \sum_j^{N_V} \frac{M_j}{eF_{V_j}} \frac{g^{V_j}_{\phi M}}{\Gamma_j} \frac{\Gamma_j M_j}{M_j^2 - q^2 - i\Gamma_j M_j}. \quad (3)$$

This parameterization integrates all the information about the meson M structure[1]. In case of radiative decay, by using the previous arguments, the amplitude is:

$$\mathcal{M}_{\rm Rad} = F_{\phi M}(0)\, \mathcal{T}_M^{\mu\nu}\, \epsilon_\mu(p) \epsilon^*_\nu(q), \quad (4)$$

[1] *E.g.*, for $M \equiv f_0$, a strong affinity of the f_0 with the $K\overline{K}$ intermediate-state (kaon loop) should manifest itself in an enhancement of the coupling $g^{\phi}_{\phi f_0}$, since in the s-channel the $K\overline{K}$ state is almost completely resonant in $\phi(1020)$.

it is constant and proportional to the value of the tff at $q^2 = 0$. To give the explicit expressions of the second-rank tensors $\mathcal{T}_M^{\mu\nu}$ we have to specify the nature of the mesons under consideration. We will study two cases

$$\mathcal{T}^{\mu\nu}_\eta = \varepsilon^{\mu\nu\rho\sigma} p_\rho q_\sigma, \qquad \mathcal{T}^{\mu\nu}_{f_0} = p^\mu q^\nu - g^{\mu\nu}(pq), \quad (5)$$

where p and q are 4-momenta as labeled in fig. 1.

The formal expressions for total annihilation cross-sections and decay rates are (eqs. (2), (5))

$$\begin{aligned} \sigma_{\phi\eta}(s) &= \rho^{\rm kin}_{\phi\eta}(s) |F_{\phi\eta}(s)|^2, \quad \Gamma_{\phi\eta} = \tau^{\rm kin}_{\phi\eta} F_{\phi\eta}(0)^2, \\ \sigma_{\phi f_0}(s) &= \rho^{\rm kin}_{\phi f_0}(s) |F_{\phi f_0}(s)|^2, \quad \Gamma_{\phi f_0} = \tau^{\rm kin}_{\phi f_0} F_{\phi f_0}(0)^2, \end{aligned} \quad (6)$$

where $s = q^2$. These quantities are products between kinematic factors ($\rho^{\rm kin}(s)$ and $\tau^{\rm kin}$), which, depending on the nature of the meson M, are different in the two cases ($M \equiv \eta$ and $M \equiv f_0$), and the modulus squared of the corresponding tff's.

3.1 Step two: selection of the contributions

In this so-called resonance region, *i.e.*, from the theoretical threshold, which is $s_0 = (3M_\pi)^2$ since the isoscalar final state, up to $\sim (3\,{\rm GeV})^2$, we adopt the parameterization of eq. (3). The first criterion used to select the vector mesons which contribute to the tff's is the quantum number conservation. For both $\phi\eta$ and ϕf_0 final state we have: $I^G(J^{PC}) = 0^-(1^{--})$, hence only contributions from the ω- and ϕ-family are expected. However, if we consider explicitly the structure of the mesons in terms of valence quarks, assuming the f_0 as $q\overline{q}$ bound state, we have

$$|\phi\rangle = s\overline{s} \qquad \begin{aligned} |\eta\rangle &= X_\eta |u,d;-\rangle + Y_\eta |s;-\rangle, \\ |f_0\rangle &= X_{f_0} |u,d;+\rangle + Y_{f_0} |s;+\rangle, \end{aligned} \quad (7)$$

with the normalization: $X^2_{\eta,f_0} + Y^2_{\eta,f_0} = 1$ and where the state $|q_1, q_2, \ldots; P\rangle$ indicates a normalized combination of $q_1\overline{q}_1$, $q_2\overline{q}_2$, etc., with parity P and $J^C = 0^+$.

While the ϕ-family contributions are allowed (fig. 2), the ω-family contributions are instead OZI-forbidden [11]. In fact, as it is shown in fig. 3, the corresponding Feynman diagrams have disconnected flavor lines in the vector sector.

It follows that, in light of the quantum number conservation and the OZI rule, only ϕ-family contributions are

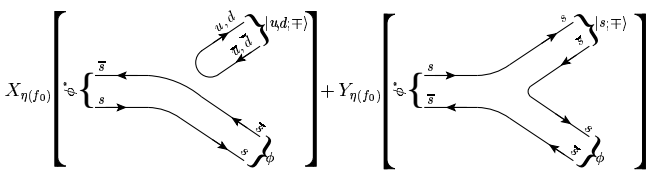

Fig. 2. Feynman diagram for $\phi^* \to \phi\eta(f_0)$ with: $|\phi\rangle = s\overline{s}$ and $|\eta(f_0)\rangle = X_{\eta,f_0}|u,d;\mp\rangle + Y_{\eta,f_0}|s;\mp\rangle$. The two components $|u,d;\mp\rangle$ and $|s;\mp\rangle$ are separately shown.

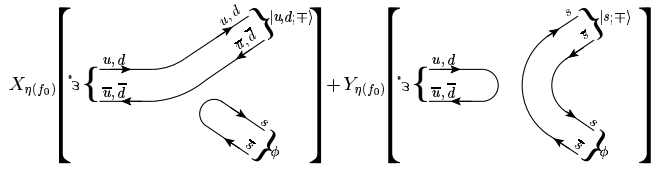

Fig. 3. Feynman diagram for $\omega^* \to \phi\eta(f_0)$ with: $|\phi\rangle = s\overline{s}$ and $|\eta(f_0)\rangle = X_{\eta,f_0}|u,d;\mp\rangle + Y_{\eta,f_0}|s;\mp\rangle$. The two components $|u,d;\mp\rangle$ and $|s;\mp\rangle$ are separately shown.

expected, not only for the $\phi\eta$, but also for ϕf_0 tff under the hypothesis of a $q\overline{q}$ f_0.

In addition, the uncertainty due to the unknown ω-ϕ mixing, allows only to reduce the $\phi\eta\gamma$ coupling with respect to $\phi f_0\gamma$. In fact, by putting $Y_\eta = 0$, it should remain the only $|u,d;-\rangle$ component, which, being OZI forbidden (see first diagram in fig. 2), should give $g^\phi_{\eta\gamma} = 0$. Contrary, by putting $Y_{f_0} = 0$, the remaining component $|u,d;+\rangle$ is a combination of u and d quarks with scalar quantum numbers ($J^{PC} = 0^{++}$) and then it is not OZI suppressed [12].

3.2 The asymptotic region

Another crucial point of this procedure is the knowledge of the time-like asymptotic behaviour of a hadronic form factor. To this purpose, the nominal power law, as predicted by the perturbative QCD (pQCD) [13], is used. The power to be considered, linearly depends on the number of elementary constituents, *i.e.* valence quarks, even though further sub-structures are present (*e.g.*: deuteron [14]).

In addition, in order to describe the asymptotic behaviour of the tff's under consideration, we have also to account for the flip of the hadronic helicity[2] [15], which passes from zero, in the leptonic initial state, to one in the $\phi\eta(f_0)$ final state ($\lambda_{\eta(f_0)} = 0$, $|\lambda_\phi| = 1$). This implies an additional suppression, and then the asymptotic behaviour to be considered, starting from a certain energy $s^{\eta(f_0)}_{\rm asy}$, is [15,16]

$$F^{\rm asy}_{\phi\eta(f_0)}(s) \propto \left(\frac{1}{s}\right)^{n_H + \frac{n_\lambda + l_q - 1}{2} = 2\left(\frac{5}{2}\right)} \qquad s > s^{\eta(f_0)}_{\rm asy}, \qquad (8)$$

where $n_\lambda = |\lambda_{\eta(f_0)} + \lambda_\phi| = 1$, $n_H = 2$, $l_q = 0(1)$. The power is a function of the number of hadronic fields n_H, the modulus of the total helicity n_λ and the relative angular momentum of the quarks which constitute the meson η ($l_q = 0$) or f_0 ($l_q = 1$). The parameterization of eq. (8) provides different asymptotic powers for $\phi\eta$ and $\phi f_0(q\overline{q})$ tff.

[2] The virtual photon of the annihilation $e^+e^- \to \gamma^* \to \phi M$, at high energies, always has spin ± 1 along the beam axis. Angular-momentum conservation implies that the total angular momentum is 1. In the center-of-mass frame: $\boldsymbol{p}_\phi = -\boldsymbol{p}_M \equiv \boldsymbol{p}$ it follows that

$$\left|\frac{\boldsymbol{p}_\phi \cdot \boldsymbol{s}_\phi}{|\boldsymbol{p}_\phi|} - \frac{\boldsymbol{p}_M \cdot \boldsymbol{s}_M}{|\boldsymbol{p}_M|}\right| = |\lambda_\phi - \lambda_M| = \left|\frac{\boldsymbol{p} \cdot \boldsymbol{s}_{\rm tot}}{|\boldsymbol{p}|}\right| = 0, 1, \qquad (9)$$

where λ_ϕ and λ_M are the helicities of the final mesons. But, since hadronic helicity conservation requires: $\lambda_\phi + \lambda_M = 0$, or $\lambda_\phi - \lambda_M = 2\lambda_\phi = -2\lambda_M$, eq. (9) holds, in case of mesons, only if $|\lambda_\phi| = |\lambda_M| = 0$. In the cases under consideration, the coupling $\gamma^*\phi M$ ($M = \eta, f_0$) is described in terms of only one tff $F_{\phi M}(s)$ and this requires $|\lambda_\phi| = 1$. Helicity zero would mean that the ϕ spin lies in the plane orthogonal to its 3-momentum, in this case we would need an additional degree of freedom (for instance: the azimuthal angle) and then an additional tff to describe this process. But since the tff is only one it follows that the ϕ spin lies in 3-momentum direction, *i.e.* $|\lambda_\phi| = 1$.

3.3 The region below the theoretical threshold s_0

Unitarity assures that a generic hadronic tff $F_H(s)$ is an analytic function in the s-complex plane with a cut, along the real axis, starting from the theoretical threshold s_0 up to infinity. This property, together with a power law vanishing asymptotic behaviour allows to use spectral representations for the tff's as, for instance, the dispersion relation (DR) for the imaginary part [17]. However, to use directly the experimental data and the asymptotic behaviour (eq. (8)) in the time-like region, we use the DR for the logarithm [18]:

$$\ln[F_H(t)] = \frac{\sqrt{s_0 - t}}{\pi} \int_{s_0}^{\infty} \frac{\ln|F_H(s)|}{(s-t)\sqrt{s-s_0}} {\rm d}s, \qquad (10)$$

which relates the real values of the tff below the theoretical threshold ($t < s_0$) to its modulus over the cut. The DR for the logarithm can be used in the form of eq. (10) only if $F_H(s)$ has neither zeros nor poles on the physical sheet. The parameterization used in the resonance region (eq. (3)) guarantees the absence of singularities for the tff's in the physical sheet.

Since we know the modulus of the tff $F_{\phi\eta(f_0)}(s)$ over the cut (eqs. (3), (8)), the DR for the logarithm allows to perform an analytic continuation of the parameterization below the theoretical threshold and it gives:

$$F^{\rm an}_{\phi\eta(f_0)}(t) = \exp\left[\frac{\sqrt{s_0 - t}}{\pi}\left(\int_{s_0}^{s^{\eta(f_0)}_{\rm asy}} \frac{\ln|F^{\rm Res}_{\phi\eta(f_0)}(s)|}{(s-t)\sqrt{s-s_0}}{\rm d}s + \int_{s^{\eta(f_0)}_{\rm asy}}^{\infty} \frac{\ln|F^{\rm asy}_{\phi\eta(f_0)}(s)|}{(s-t)\sqrt{s-s_0}}{\rm d}s\right)\right], \quad t < s_0. \qquad (11)$$

3.4 The overall parameterization

We are now ready to write down the parameterization which covers the whole s-real axis (in principle the whole s-complex plane), it is a three-fold definition:

$$F_{\phi\eta(f_0)}(s) = \begin{cases} F^{\rm an}_{\phi\eta(f_0)}(s) & s \le s_0 \qquad \text{(eq. (11))}, \\ F^{{\rm Res}(\phi)}_{\phi\eta(f_0)}(s) & s_0 < s \le s^{\eta(f_0)}_{\rm asy} \qquad \text{(eq. (3))}, \\ F^{\rm asy}_{\phi\eta(f_0)}(s) & s > s^{\eta(f_0)}_{\rm asy} \qquad \text{(eq. (8))}. \end{cases} \qquad (12)$$

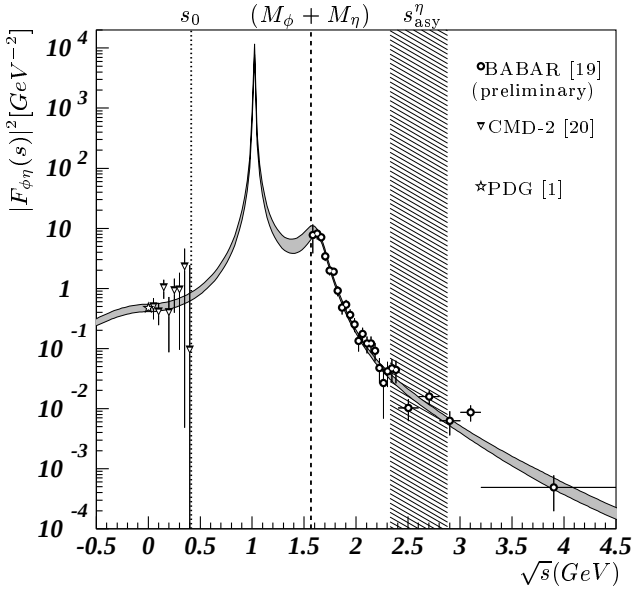

Fig. 4. Reconstructed $|F_{\phi\eta}(s)|^2$ tff. The grey band represents the error. The circles are the preliminary BABAR data used as input, while the triangles (CMD-2: $\phi \to \eta e^+e^-$) and the star (PDG: $\phi \to \eta\gamma$) are not included in the computation. The dotted and the dashed vertical lines represent the theoretical and the physical thresholds, and the lined region in the obtained interval for $s^\eta_{\rm asy}$.

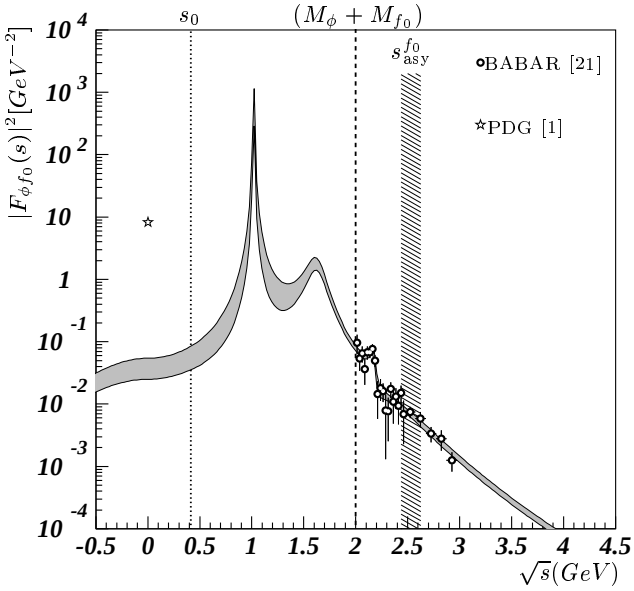

Fig. 5. Reconstructed $\phi f_0(q\overline{q})$ tff. The grey band represents the error. The circles are the BABAR data used as input, while the star (PDG: $\phi \to f_0\gamma$) is not included in the computation. The dotted and the dashed vertical lines represent the theoretical and the physical thresholds, and the lined region in the obtained interval for $s^{f_0}_{\rm asy}$.

Table 1. Parameters obtained for the $\phi\eta$ tff. The values without error are fixed.

Res	$g^V_{\phi\eta}(\mathrm{GeV}^{-1})$	$M_V(\mathrm{MeV})$	$\Gamma_V(\mathrm{MeV})$
ϕ	13 ± 1.4	1019.4	4.3
ϕ'	56 ± 6	1622 ± 15	203 ± 12

The real axis has been divided into three intervals to parameterize the tff. From higher energies: the asymptotic region, where the pQCD power law is used with power 2 for the η and 5/2 for the $f_0(q\overline{q})$; the resonance region, where the tff is written in terms of vector propagators and coupling constants; the analytic region, where the tff is reconstructed by means of a DR.

4 The $\phi\eta$ transition form factor

In fig. 4 the reconstructed $\phi\eta$ tff is shown. This result has been obtained by considering only ϕ-family contributions in the resonance region, namely the $\phi(1020) \equiv \phi$ and $\phi(1680) \equiv \phi'$, and a power law asymptotic behaviour $\propto (1/s)^2$. Higher-mass resonances are not included because their effect in the low-energy region under consideration is negligible.

By using only the BABAR data (circles in fig. 4) and the analyticity to fix the free parameters of the procedure, the function defined in eq. (12) reproduces the low-energy behaviour of the tff in good agreement with the data. The obtained parameters are shown in table 1.

Table 2. Parameters obtained in the case of the $\phi f_0(q\overline{q})$ tff. The additional resonance ϕ'' is included by hand [21]. The values without error are fixed.

Res	$g^V_{\phi f_0}(\mathrm{GeV}^{-1})$	$M_V(\mathrm{MeV})$	$\Gamma_V(\mathrm{MeV})$
ϕ	3.5 ± 0.9	1019.4	4.3
ϕ'	26 ± 3	1622	203
ϕ''	$F_{\phi''}(6.4 \pm 0.3) \cdot 10^{-3}/M_{\phi''}$	2176	51

By using eq. (6) we get: $BR(\phi \to \eta\gamma) = (1.3 \pm 0.2)\%$, to be compared with [1]: $BR_{\rm PDG}(\phi \to \eta\gamma) = (1.301 \pm 0.024)\%$ (see fig. 4). This good agreement provides an important positive check for two key points of the procedure *i.e.*, the description in terms of resonances in the low-energy region and the power law asymptotic behaviour.

5 The $\phi f_0(q\overline{q})$ transition form factor

In fig. 5 is shown the reconstructed $\phi f_0(q\overline{q})$ tff, under the hypothesis of a $q\overline{q}$ f_0 and the corresponding parameters are reported in table 2. This result has been obtained with the same prescriptions used in the previous $\phi\eta$ case, *i.e.* by considering only ϕ-family contributions (here there is also the ϕ'' [21]) and a $(1/s)^{5/2}$ asymptotic power law (eq. (8)).

In this case we get: $BR(\phi \to f_0\gamma) = (2.1 \pm 0.8) \cdot 10^{-6}$, while: $BR_{\rm PDG}(\phi \to f_0\gamma) = (4.40 \pm 0.21) \cdot 10^{-4}$ [1]. We stress that this result has been obtained assuming for the f_0 a quark structure identical to that of the η (eq. (7)).

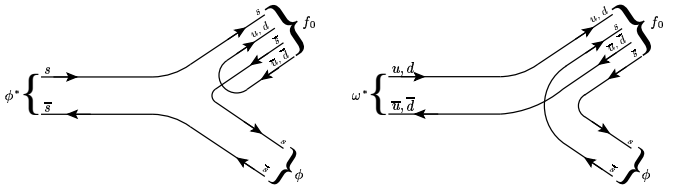

Fig. 6. Feynman diagrams for the ϕ^* and ω^* contribution to the ϕf_0 final state with a tetraquark f_0.

6 The $\phi f_0(qq\overline{qq})$ transition form factor

To account for an f_0 with a tetraquark structure like: $(ns\overline{ns})$, where $n = u, d$, two steps in our procedure need improvement.

The first upgrade concerns the resonance region, where the tetraquark structure allows both the ϕ- and ω-family contributions (see fig. 6), which were previously forbidden. The second is about the asymptotic behaviour. Since the pQCD asymptotic power depends on the number of hadronic fields, an additional valence quark implies a further factor $(1/s)$ and, having the two pairs qq and $\overline{qq}$ zero relative angular momentum and total spin [22], there is no more the $l_q = 1$ attenuation and the asymptotic power becomes: $p(n_H = 3, n_\lambda = 1, l_q = 0) = 3$.

The new overall parameterization is

$$F_{\phi f_0(qq\overline{qq})} = \begin{cases} F^{\rm an}_{\phi f_0}(s), & s \le s_0, \\ F^{{\rm Res}(\phi,\omega)}_{\phi f_0}(s), & s_0 < s \le s^{f_0}_{\rm asy}, \\ \propto s^{-3}, & s > s^{f_0}_{\rm asy}, \end{cases} \qquad (13)$$

where the only $\omega(782)$ has been included in the region $]s_0, s^{f_0}_{\rm asy}]$ (higher mass ω-recurrences have no important effects) and a faster vanishing asymptotic behaviour is implemented for $s > s^{f_0}_{\rm asy}$.

6.1 Results for $f_0(qq\overline{qq})$

In fig. 7 is shown the ϕf_0 tff obtained under the hypothesis of a tetraquark f_0 and the corresponding parameters are reported in table 3. In this scenario our prediction for the tff, which gives: $BR(\phi \to f_0\gamma) = (3.9 \pm 0.9) \cdot 10^{-4}$ is in good agreement with the PDG value (mainly due to KLOE [23]), which is: $BR_{\rm PDG}(\phi \to f_0\gamma) = (4.40 \pm 0.21) \cdot 10^{-4}$.

This drastic change in the low-energy result, with respect to the previous case without the ω, is the consequence of a combined effect of the two modifications; the faster vanishing asymptotic behaviour enhances the resonance region and the additional ω contribution moves, down in energy, its mean value. The sum of these two effects is just a large enhancement of the tff at $s = 0$.

7 Duality

The pQCD nominal power law of eq. (8) behaves like a counter of valence quarks involved in a certain process.

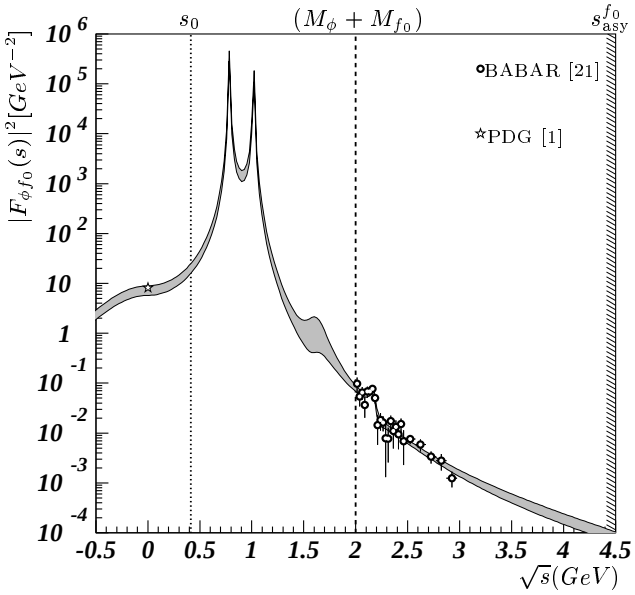

Fig. 7. Reconstructed $\phi f_0(qq\overline{qq})$ tff. The grey band represents the error. The circles, on the right, are the BABAR data used as input, while the star (PDG: $\phi \to f_0\gamma$) is not included in the computation. The dotted and the dashed vertical lines represent the theoretical and the physical thresholds, and the lined region in the obtained interval for $s^{f_0}_{\rm asy}$.

Table 3. Parameters obtained in the case of the $\phi f_0(qq\overline{qq})$ tff. The values without error are fixed.

Res	$g^V_{\phi f_0}(\mathrm{GeV}^{-1})$	$M_V(\mathrm{MeV})$	$\Gamma_V(\mathrm{MeV})$
ω	112 ± 13	783.7	8.5
ϕ	52 ± 7	1019.4	4.3
ϕ'	12 ± 7	1622	203
ϕ''	$F_{\phi''}(1.9 \pm 0.4) \cdot 10^{-3}/M_{\phi''}$	2176	51

Nevertheless, there is an objective difficulty in exploiting experimentally this power counting. In fact, the high-energy values of the tff's, due to their power law vanishing, are by definition very small quantities. In the low-energy region, where the tff's attain their higher values and then the experimental observation should be more feasible, the power law behaviour is covered by the resonances.

However, following the so-called quark-hadron duality [24], the asymptotic behaviour may be "restored" also at low energy by averaging the tff's and then by canceling the local effects of the resonances.

Figure 8 shows the asymptotic powers of the $\phi\eta$, ϕf_0 tff's and also of the pion form factor $F_{\pi\pi}(s)$, which is used as a check of the averaging procedure. The results are in agreement with the expectations and they confirm the further suppression due to the helicity flip in case of $F_{\phi\eta}(s)$ (first experimental observation) and the additional hadronic filed in case of $F_{\phi f_0}(s)$.

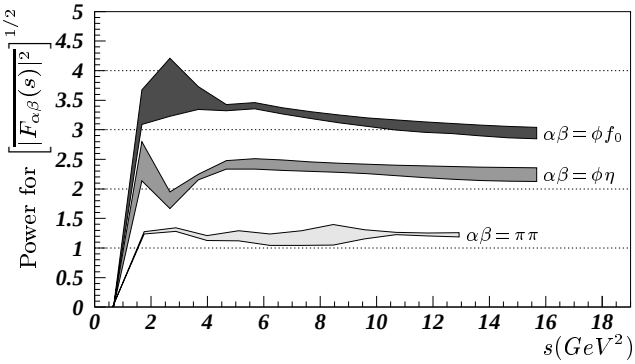

Fig. 8. Asymptotic powers for the mean values of $\pi\pi$ form factor (light-grey band) and, the $\phi\eta$ (medium-grey band) and ϕf_0 (dark-grey band) tff's.

8 Conclusions

We have defined a dispersive technique to construct, for a generic ϕM tff, an analytic parameterization which is defined in the whole s-complex plane (M is a pseudoscalar or scalar light meson). The main ingredients of this technique are: the pQCD counting rule [13] (and helicity rule [15]) to describe the asymptotic behaviour; data on the annihilation cross-section $\sigma(\phi M)$; Breit-Wigner parameterization in the resonance region and DR's for the logarithm.

In the case of the $\phi\eta$ tff, by considering only the ϕ-family contributions, assuming the asymptotic behaviour $(1/s^2)$, and using the BABAR data on $\sigma(\phi\eta)$, we achieved a parameterization $F_{\phi\eta}(s)$ (fig. 4), which is in good agreement with the low energy data, not used in the analysis.

In the case of the ϕf_0 tff, the same procedure, *i.e.*, an analysis under the hypothesis of a $q\overline{q}$ f_0 with the opportune $(1/s^{5/2})$ asymptotic behaviour, gives a prediction in huge disagreement with the low-energy data (fig. 5).

We modified the procedure in order to account for a tetraquark f_0. The modification concerns two steps: a new contribution coming from the ω-family is included; the asymptotic behaviour becomes $(1/s^3)$ because of the additional quarks in the final state and the disappearing of the angular momentum attenuation. These two upgrades, if individually considered, give opposite effects: the first reduces, while the second enhances the low-energy values of the tff. However, the combined effect gives an important enhancement of the tff, which reconciles the prediction with the data (fig. 7).

In addition, we have performed an analysis in terms of quark-hadron duality, which, by restoring the power law behaviour at low energy, allows to extract the asymptotic power from the data and the parameters of the resonances. The results are in good agreement with a tetraquark f_0 and with the helicity rule, which is for the first time experimentally confirmed.

Since, by means of this procedure we have tested two extreme hypotheses concerning the f_0 structure, *i.e.* the two- and the four-quark state, our conclusion is that: the available data, the analyticity requirement and the pQCD asymptotic behaviour prove that the tetraquark component in the f_0 is the dominant one.

A still in progress analysis, where both the components are included, gives for the $q\overline{q}$ content an upper limit of 12%. It follows that the four-quark state represents at least the 88% of the f_0 structure.

I warmly acknowledge R. Baldini, G. Isidori, L. Maiani, G. Pancheri and A. Polosa for precious discussions on the subject of this talk and, BABAR and KLOE Collaborations for support and cooperation.

References

1. W.-M. Yao *et al.*, J. Phys. G **33**, 1 (2006).
2. E. Klempt, arXiv:hep-ph/0404270.
3. N.N. Achasov, V.V. Gubin, Phys. Rev. D **63**, 094007 (2001); V.E. Markushin, Eur. Phys. J. A **8**, 389 (2000) (arXiv:hep-ph/0005164); J.A. Oller, Phys. Lett. B **426**, 7 (1998) (arXiv:hep-ph/9803214); E. Marco, S. Hirenzaki, E. Oset, H. Toki, Phys. Lett. B **470**, 20 (1999) (arXiv:hep-ph/9903217); J.A. Oller, Nucl. Phys. A **714**, 161 (2003) (arXiv:hep-ph/0205121).
4. M. Boglione, M.R. Pennington, Eur. Phys. J. C **30**, 503 (2003) (arXiv:hep-ph/0303200).
5. L. Maiani, F. Piccinini, A.D. Polosa, V. Riquer, Phys. Rev. Lett. **93**, 212002 (2004) (arXiv:hep-ph/0407017).
6. G. Isidori, L. Maiani, M. Nicolaci, S. Pacetti, JHEP **0605**, 049 (2006) (arXiv:hep-ph/0603241).
7. R.L. Jaffe, Phys. Rep. **409**, 1 (2005) (Nucl. Phys. Proc. Suppl. **142**, 343 (2005)) (arXiv:hep-ph/0409065).
8. F.E. Close, AIP Conf. Proc. **717**, 919 (2004) (arXiv:hep-ph/0311087).
9. N.N. Achasov, V.N. Ivanchenko, Nucl. Phys. B **315**, 465 (1989); S. Nussinov, T.N. Truong, Phys. Rev. Lett. **63**, 1349 (1989); **63**, 2002 (1989)(E); J.L. Lucio Martinez, J. Pestieau, Phys. Rev. D **42**, 3253 (1990); F.E. Close, N. Isgur, S. Kumano, Nucl. Phys. B **389**, 513 (1993) (arXiv:hep-ph/9301253); N. Brown, F.E. Close, *The DNE Physics Handbook*, edited by L. Maiani, G. Pancheri, N. Paver (INFN, Frascati, 1995) pp. 447-464.
10. KLOE Collaboration (F. Ambrosino *et al.*), Phys. Lett. B **634**, 148 (2006) (arXiv:hep-ex/0511031).
11. G. Zweig, CERN report S419/TH412 (1964) unpublished; S. Okubo, Phys. Lett. **5**, 165 (1963); I. Iizuka, K. Okuda, O. Shito, Prog. Theor. Phys. **35**, 1061 (1966).
12. P. Geiger, N. Isgur, Phys. Rev. D **47**, 5050 (1993); S. Descotes-Genon, L. Girlanda, J. Stern, JHEP **0001**, 041 (2000) (arXiv:hep-ph/9910537); N. Isgur, H.B. Thacker, Phys. Rev. D **64**, 094507 (2001) (arXiv:hep-lat/0005006).
13. S.J. Brodsky, G.R. Farrar, Phys. Rev. D **11**, 1309 (1975).
14. S.J. Brodsky, B.T. Chertok, Phys. Rev. D **14**, 3003 (1976).
15. S.J. Brodsky, G.P. Lepage, Phys. Rev. D **24**, 2848 (1981). S.J. Brodsky, G.F. de Teramond, Phys. Lett. B **582**, 211 (2004) (arXiv:hep-th/0310227).
16. V.L. Chernyak, A.R. Zhitnitsky, Phys. Rep. **112**, 173 (1984); V. Chernyak, arXiv:hep-ph/9906387; G.R. Farrar, D.R. Jackson, Phys. Rev. Lett. **35**, 1416 (1975).
17. See for instance: E.C. Tichmarsch, *The Theory of Functions* (Oxford University Press, London, 1939).
18. B.V. Geshkenbein, Yad. Fiz. **9**, 1232 (1969).
19. BABAR Collaboration (A. Zallo), private comunication.

20. M.N. Achasov, V.M. Aulchenko, K.I. Beloborodov, A.V. Berdyugin, Phys. Lett. B **504**, 275 (2001).
21. BABAR Collaboration (G. Solodov), *Initial state radiation study at BABAR and the application to the R measurement and hadron spectroscopy*, talk presented at *ICHEP 06, Moscow, Russia*.
22. R.L. Jaffe, Phys. Rev. D **15**, 267 (1977).
23. KLOE Collaboration (A. Aloisio *et al.*), Phys. Lett. B **537**, 21 (2002) (arXiv:hep-ex/0204013).
24. J.J. Sakurai, Phys. Lett. B **46**, 207 (1973).